Modern Physics Letters B, Vol. 16, Nos. 23 & 24 (2002) 889–894

ARTIFICIAL METAL NANOCLUSTER CRYSTALS

JIN-FENG JIA, X. LIU, S. C. LI, J. Z. WANG, J. L. LI, H. LIU,
M. H. PAN, R. F. DOU and QI-KUN XUE

State Key Laboratory for Surface Physics, Institute of Physics,
Chinese Academy of Sciences, Beijing 100080, China

ZHI-QIANG LI

Steacie Institute for Molecular Sciences, National Research Council of Canada,
Ottawa, Ontario, K1A 0R6, Canada

S. B. ZHANG

National Renewable Energy Laboratory, Golden, CO 80401, USA

Received 17 June 2002

Artificial metal nanocluster crystals, (i.e. periodic lattices consisting of identical metal nanoclusters) were fabricated using a novel technique in which surface mediated magic clustering was used to achieve identical cluster size, while the Si(111)-7 × 7 surface was used as a template for ordering the clusters. The universality of this strategy was demonstrated by fabricating more than 10 different nanocluster arrays with different metals and alloys. The atomic structures, formation mechanism and stability of the nanoclusters were studied with *in situ* scanning tunneling microscopy combined with first-principles total energy calculations. Our study shows that delicate control of growth kinetics is extremely important for cluster crystal fabrication.

1. Introduction

The fabrication and the understanding of nanoclusters have recently become exciting areas of research[1–11] owing to their tremendous potential in technology applications and scientific importance in bridging our understanding between molecular and condensed matter physics. The properties of nanoclusters are size- and composition-specific, so it is possible to design materials with desired properties by choosing the correct size and composition of clusters. Their special properties may, however, be degraded by the inhomogeneity in nanocluster materials with broad size distribution and random spatial arrangements. It therefore becomes critical (for their practical application) to fabricate stable, ordered, and identical-sized nanocluster arrays. In many aspects, nanoclusters are artificial atoms,[9,12] so a periodic lattice made up of the clusters of the same nanometer size is an artificial crystal. This new form of condensed matter provides unprecedented opportunities for exploring the laws of physics. Self-organization in heterogeneous strained thin

film growth[13,14] and self-assembly in chemical synthesis[6,11] are two of the most commonly used methods to obtain such nanostructures. However, none of these methods has succeeded in producing identical nanodots with periodic spatial distributions, which are highly desired for practical device engineering.

In this work, a novel technique, in which surface-mediated magic clustering is used to achieve the identical dot size, while the Si(111)-7 × 7 surface is used as a template for positioning them in order, was developed to fabricate the artificial nanocluster crystals.[15–17] The atomic structures, formation mechanism and stability of the nanoclusters were studied with *in situ* scanning tunneling microscopy observation combined with first-principles total energy calculations.

2. Experimental Details

The experiments were carried out with an OMICRON variable temperature STM operated in ultrahigh vacuum (base pressure $\sim 5 \times 10^{-11}$ Torr).[18–20] The samples were heated by passing electric currents directly through them, and the sample temperatures were monitored by an infrared pyrometer. The Si(111) samples (as doped, 0.1 ohm cm) were cleaned by flashing to ~ 1200°C, while keeping the vacuum better than 1×10^{-9} mbar. Well-ordered Si(111)-7 × 7 surfaces can normally be obtained after cleaning. Boron nitride crucibles were used to produce Al, Ga, In (purity 99.9999%) and Mn (purity 99.9%) atomic beams. Ag and Pb deposition was performed by direct current heating in a tungsten bracket filament. A chemically etched tungsten tip was used as the STM probe. All STM images reported here were recorded in the constant current mode with a tunneling current of 20 to 100 pA.

3. Results and Discussion

Figure 1(a) shows a large scale STM image of the ordered Al cluster array on the Si(111)-7 × 7 substrate. We can clearly see that the cluster array is very uniform in this large area. Larger area scans and scans at different locations reveal that the cluster array is even uniform over the whole sample surface ($\sim 2 \times 9$ mm^2). A zoom-in STM image (at negative sample bias) is shown in Fig. 1(b). Each bright spot in the image corresponds to an Al cluster. Except for some inhomogeneities caused by defects or locally over-deposited Al, the ordering of the clusters is essentially perfect. The Al clusters equally occupy both halves of the Si(111)-7 × 7 unit cell forming a characteristic honeycomb structure. Considering each cluster as an artificial atom, this periodic lattice of the same-sized clusters represents a new artificial crystal, and the geometry of this "lattice" is the same as that of the Si(111)-7 × 7.

In the high resolution STM image (Fig. 1(c)), the Al clusters appear triangular and reside at the center of each half of the Si(111)-7 × 7 unit cell. Each cluster contains six bright spots, the three on the edge are brighter than those at the corner. The distance between two edge spots is (5.5±0.5) Å; while the distance between the corner spot and neighboring edge spot is (4.6±0.5) Å. The empty-state STM image

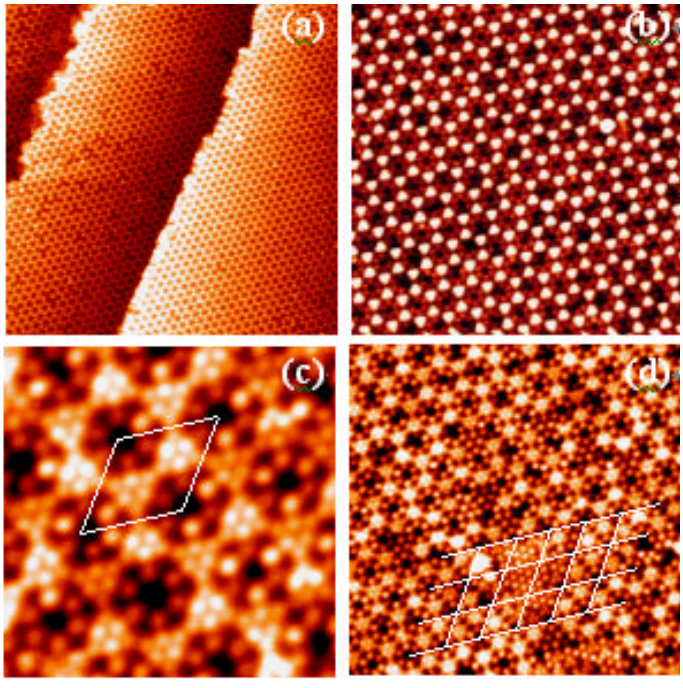

Fig. 1. (a) Perfectly ordered Al nanocluster array at $\sim$ 0.25 ML Al coverage. The image was obtained at Vs = 2.0 V. The image size is (100 × 100) nm (deposition rate $\sim$ 0.01 ML/min at temperature $\sim$ 300°C). (b) Close-up view of the Al nanoclusters array in (b). Vs = −2.0 V. The image size is (30 × 30) nm. (c) Atomically resolved STM image (10 × 10) nm of the Al clusters recorded at +1.1 V. (d) Coexistence of Si(111)-$\sqrt{3} \times \sqrt{3}$-Al, -$\sqrt{7} \times \sqrt{7}$-Al and Al nanoclusters after annealing the sample in (b) at about 550°C. The image size is (25 × 25) nm and Vs = 1.2 V.

of the Al cluster is very similar to that of the Ga cluster.[17] However, it is different from that of the In cluster where the three spots on the edges of the triangle appear darker.[15–17]

In addition, the Al nanocluster array is stable and can survive even at an annealing temperature up to 500°C. After annealing the Al nanocluster array (shown in Figs. 1(b) and (c)) at about 550°C, small areas of $\sqrt{3} \times \sqrt{3}$-Al and $\sqrt{7} \times \sqrt{7}$-Al appear and coexist with the Al nanoclusters, as shown in Fig. 1(d). According to the atomic structure models of the Si(111)-$\sqrt{3} \times \sqrt{3}$-Al and -$\sqrt{7} \times \sqrt{7}$-Al, each $\sqrt{3} \times \sqrt{3}$ unit cell contains one Al atom, while the $\sqrt{7} \times \sqrt{7}$ unit cell has three Al atoms.[21] Assuming that all Al atoms forming the $\sqrt{3} \times \sqrt{3}$-Al or the $\sqrt{7} \times \sqrt{7}$-Al reconstruction come from the clusters in the same area (this is true as no noticeable change in the surrounding areas was observed), the number of the total Al atoms in the reconstruction area can be easily calculated. With this simple method, each Al cluster is determined to contain (6 ± 0.3) Al atoms.

First-principles total energy calculations were performed to investigate the atomic structure and formation mechanism of the Al clusters. Starting from the

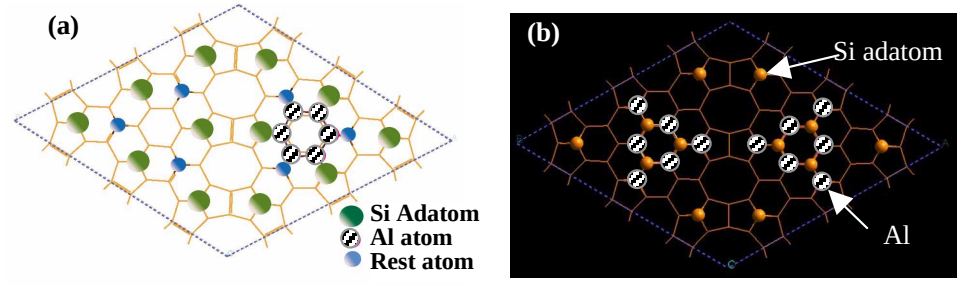

Fig. 2. (a) Top view of the honeycomb atomic structure model proposed for the Al six-atom cluster. (b) Top view of the atomic structure established for the In/Ga/Al cluster in this work. The big hatched balls are Al atoms and the small solid balls are Si adatoms.

STM observation and coverage measurement, we calculated the formation energies of three possible structure models: (i) three-Al-atom cluster within the triangle defined by the three Si rest atoms, (ii) six-Al-atom cluster forming a hexagonal ring (Fig. 2(a)), and (iii) six-Al-atom cluster forming a hollow-centered triangle (Fig. 2(b)). It is found that the optimized structure is the Al6 model, as demonstrated in Fig. 2(b). In this model six threefold-coordinated Al form a triangle and three Si adatoms originally on the edge are displaced towards the triangle center considerably (Fig. 2(b)). So, the three Si adatoms originally on the edge and the three Si rest atoms become fourfold-coordinated, removing six dangling bonds from each 7×7 unit cell. The simulated STM image based on this conformation agrees well with the experiment.[16,17]

To test the generality of the method, we studied several different systems. These systems have been investigated previously, and there is no report on the formation of such ordered cluster array. The growth conditions are very important for such nanocluster formation, and the window is very narrow, which is probably the most important reason why these nanoclusters were not found in previous studies. The universality of this strategy is demonstrated by our success in fabricating more than 10 different nanocluster arrays with different metals and alloys, including Al, Ga, In, Pb, Mn, Ag, In/Mn and Ag/In. In Fig. 3, we show a library of 12 different patterns of perfectly-ordered, highly uniform In, Ga, Ag, Mn and Co cluster arrays on Si(111) fabricated using this method.[15–17,19] We note that

(i) all the ordered cluster arrays shown here are stable at temperatures up to 200°C. This feature is to be contrasted with metal clusters formed on metal surfaces, which are typically stable only at low temperatures (e.g. up to 150 K for Ag nanoclusters on Pt(111)[14]);
(ii) there is no fundamental limitation on fabricating identical-size clusters.

Thus, upon further improvement the present approach can be made precise and practical in fabricating perfectly ordered identical-size cluster arrays. We further emphasize that our approach is not limited to Si. It applies as long as the substrate

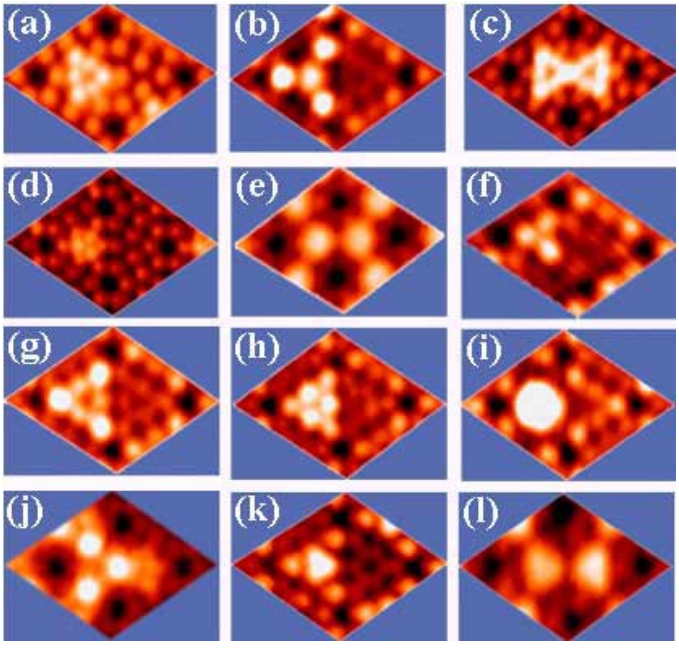

Fig. 3. An image library showing the appearance and spatial arrangement of 12 different nanocluster arrays (only one 7×7 unit cell is shown). (a) In6 cluster, (b) In9 cluster, (c) two In6 clusters in a honey-comb structure, (d) Ga6 cluster, (e) Ga6 clusters in a honey-comb structure, (f) Ag3 cluster, (g) Ag6 cluster, (h) Ag9 cluster, (i) Ag12 cluster, (j) In12 + Cox cluster in a honey-comb structure, (k) In6 + Ag3 cluster, and (l) In6 + Mn3 cluster.

template used to accumulate and separate these building blocks exists or can at least be prepared.

4. Conclusion

In this work, high-quality artificial metal nanocluster crystals were fabricated on Si(111)-7×7 by a novel method involving surface-mediated magic clustering. The atomic structure and formation mechanism of Al clusters were investigated by STM and first-principles total energy calculations. It is found that delicate control of the growth kinetics is very important to achieving successful results. We would point out that there is essentially no limitation to this strategy. High stability and unique structure of these nanocluster crystals provide unprecedented opportunities for exploring new physical phenomena and applications.

Acknowledgment

Supported by China NSF (60021403, 10134030, 10174089, 60128404). Work at NREL was supported by U. S. DOE/OS/BES under contract No. DE-AC36-99GO10337.

References

1. M. Valden, X. Lai and D. W. Goodman, *Science* **281**, 1647 (1998).
2. M. Haruta, *Catal. Today* **36**, 153 (1997).
3. A. O. Orlov, I. Amlani, G. H. Bernstein, C. S. Lent and G. L. Snider, *Science* **277**, 928 (1997).
4. R. P. Andres, T. Bein, M. Dorogi, S. Feng, J. I. Henderson, C. P. Kubiak, W. Mahoney, R. G. Osifchin and R. Reifenberger, *Science* **272**, 1323 (1996).
5. T. W. Kim, D. C. Choo, J. H. Shim and S. O. Kang, *Appl. Phys. Lett.* **80**, 2168 (2002).
6. S. Sun C. B. Murray, D. Weller, L. Folks and A. Moser, *Science* **287**, 1989 (2000).
7. K. Koike, H. Matsuyama, Y. Hirayama, K. Tanahashi, T. Kanemura, O. Kitakami and Y. Shimada, *Appl. Phys. Lett.* **78**, 874 (2001).
8. T. Koide, H. Miyauchi, J. Okamoto, T. Shidara, A. Fujimori, H. Fukutani, K. Amemiya, H. Rakeshita, S. Yuasa, T. Katayama and Y. Suzuki, *Phys. Rev. Lett.* **87**, 257201 (2001).
9. P. M. Petroff, A. Lorke and A. Imamoglu, *Phys. Today* **46**, May (2001).
10. V. F. Puntes, K. M. Krishnan and A. P. Alivisatos, *Science* **291**, 2115 (2001).
11. C. T. Black, C. B. Murray, R. L. Sandstrom and S. H. Sun, *Science* **290**, 1131 (2000).
12. P. L. McEuen, *Science* **278**, 1729 (1997).
13. K. Bromann, C. Félix, H. Brune, W. Harbich, R. Monot, J. Buttet and K. Kern, *Science* **274**, 956 (1996).
14. H. Brune, M. Glovannini, K. Bromann and K. Kern, *Nature* **394**, 451 (1998).
15. J. L. Li, J. F. Jia, X. J. Liang, X. Liu, J. Z. Wang, Q. K. Xue, Z. Q. Li, J. S. Tse, Z. Y. Zhang and S. B. Zhang, *Phys. Rev. Lett.* **88**, 066101 (2002).
16. J. F. Jia, J. Z. Wang, X. Liu, Q. K. Xue, Z. Q. Li, Y. Kawazoe and S. B. Zhang, *Appl. Phys. Lett.* **80**, 3186 (2002).
17. J. F. Jia, X Liu, J. Z. Wang, J. L. Li, X. S. Wang, Q. K. Xue, Z. Q. Li, Z. Y. Zhang and S. B. Zhang, *Phys. Rev.* **B66** (in press).
18. J. L. Li, X. J. Liang, J. F. Jia, X. Liu, J. Z. Wang, E. G. Wang and Q. K. Xue, *Appl. Phys. Lett.* **79**, 2826 (2001).
19. J. F. Jia, J. L. Li, X. J. Liang, X. Liu, J. Z. Wang, H. Liu, R. F. Dou, M. J. Xu, M. H. Pan, S. C. Li, Q. K. Xue, Z. Q. Li, J. S. Tse, Z. Y. Zhang and S. B. Zhang, *J. Chin. Electr. Microscopy Soc.* **21**, 270 (2002).
20. J. F. Jia, Q. K. Xue and S. B. Zhang, *Physics* **31**, 265 (2002) (in Chinese).
21. R. J. Hamers, *Phys. Rev.* **B40**, 1657 (1989).